Supporting Online Information

Timescales of membrane fusion revealed by direct imaging of vesicle fusion with high temporal resolution

Christopher K. Haluska, Karin A. Riske, Valérie Marchi-Artzner, Jean-Marie Lehn, Reinhard Lipowsky, and Rumiana Dimova

This *Supporting Text* contains details about the two experimental fusion protocols, part of the dimensional analysis for the time scales that govern the opening of the fusion neck in the early and later stages, the description of the four supporting movies, and the chemical structure of the ligand used in the ligand-mediated fusion protocol. The *Supporting Movies* display the time evolution of single fusion events obtained from two protocols: (*i*) fusion of vesicles that are functionalized with fusogenic ligands (Movies S1 and S2), and (*ii*) electrofusion (Movies S3 and S4).

Fusion protocol for functionalized membranes.

After electroformation, the vesicle solution was diluted in glucose and placed in a specially designed chamber consisting of two glass slides and Teflon spacers. The chamber was open in order to provide space for the insertion of several micropipettes. The pipettes were prepared from borosilicate capillaries (World Precision Instruments, USA, internal diameter of 1 mm) using a horizontal pipette puller (Sutter Instruments, USA). The internal radius of the pipettes used to manipulate the vesicles was approximately 5 μm. They were connected with Teflon tubes to a hydrostatic pressure system, which creates a small suction pressure of a few Pa inside the glass capillary. This underpressure is sufficient to aspirate and hold a vesicle. Two vesicles without visible defects were selected and brought into contact using two micropipettes. A third pipette with a smaller radius of about 1 μm was used for local injection of $EuCl_3$. The injection volumes were controlled using a picoinjector PLI100 (Harvard Apparatus, USA). Using glucose at different concentrations, the osmolarity of the $EuCl_3$ solutions was adjusted (using osmometer Osmomat030 Gonotec, Germany) in order to avoid osmotic swelling or shrinking of the vesicles. The concentration of the injected $EuCl_3$ was varied between 1 μM and 1 mM.

Electrofusion protocol.

The electroformed vesicles were diluted in glucose solution containing NaCl of concentration between 0 and 1 mM, and placed in an observation chamber (Eppendorf, Germany) with two electrodes spaced at a distance of 475±5 μm. The vesicles stayed at the bottom of the chamber because the interior sugar solution had a somewhat larger density. An alternating electric field was switched on for a short time period of about 10 s before the DC pulse was applied. The AC field aligns the vesicles along the direction of the field and brings them into contact. To some extent, this initial AC field plays the role of the micropipettes in the first protocol since it is used to position the vesicle couples. After two vesicles have come into contact, a short rectangular DC pulse is applied, which perturbs the vesicles in the contact area and induces their fusion. The DC pulse was generated using an electric field generator Multiporator (Eppendorf, Germany). Its amplitude was varied between 50 and 200 V (1±0.2 to 4±0.4 kV/cm) and its duration between 50 and 250 μs.

The vesicles were observed to drift laterally which indicated that they did not adhere to the glass surface.

The salt concentrations used in this work are substantially below physiological conditions. Concentrations higher than those used here are expected to shorten the time of membrane charging, τ_{charg}, since the media conductivity would be increased. Indeed, the charging time is given by (1)

$$\tau_{charg} = R\, C_m\, [1/\lambda_{in} + 1/(2\lambda_{out})] \qquad \text{Eq. 1}$$

where C_m is the membrane capacitance, and λ_{in} and λ_{out} are the conductivities inside and outside the vesicle, respectively. Shorter charging times would lead to an increase in the transmembrane potential V_m, which depends on time t according to (1)

$$V_m = 1.5R \cos\theta\, E\left(1 - e^{-t/\tau_{charg}}\right) \qquad \text{Eq.2}$$

where R is the vesicle radius, E the applied electric field, and θ the angle between the electric field and the vesicle surface normal.

Dimensional analysis for the early and the later stages of fusion neck expansion.

The two stages of the fusion process, a very fast early stage and a slower later stage, are detected for both fusion protocols. This is clearly observed when the diameter of the fusion neck is plotted versus time using a linear time scale as shown in Fig. 5. The latter figure contains the same data as in Fig. 3 where a logarithmic time scale is used.

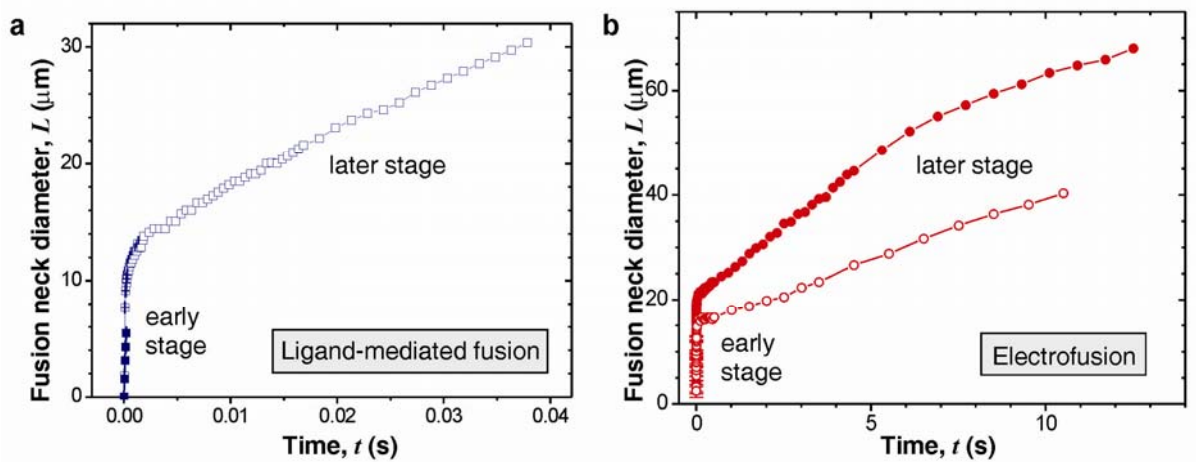

FIG. 5 Two stages in the opening of the fusion neck. The fusion neck diameter, L, as a function of time, t, plotted for (a) ligand-mediated fusion and (b) electofusion. The data are identical to those plotted in Fig. 3 in the manuscript, but here they are displayed in linear time scale.

During the early stage, the fusion neck opens very rapidly: the expansion velocity of the rim of the neck is of the order of 4 cm/s. The fusion pore has opened up to micrometers within a hundred microseconds. Intuitively, one would relate this time, τ_{early}, to fast relaxation of the membrane tension. The tension of the vesicles achieved before fusion is in the stretching regime of the membrane. Thus, τ_{early} should be primarily governed by the relaxation of membrane stretching. The viscous dissipation can be associated with two contributions: in-plane dilatational shear as the fusion neck expands and intermonolayer slip between the two leaflets of the bilayer in the zone of the fusion neck. The second is negligible for diameter of the fusion neck L larger than half a micron (2). Thus, $\tau_{early} \sim \eta_s/\sigma$, where η_s is the surface dilatational viscosity of the bilayer ≈ 0.35 N.s/m (3) (η_s has units [bulk viscosity] × [membrane thickness]). For membrane tensions of the order of 5 mN/m, which should be close to the tension of rupture, one obtains $\tau_{early} \sim \eta_s/\sigma \sim 100$ μs in agreement with the experimental observations from which we deduced 300 μs as the appropriate time scale in order to complete the early stage of fusion.

During the later stage of the fusion process, the neck expansion velocity slows down by two orders of magnitude. Here the dynamics is mainly governed by the displacement of the volume ΔV of fluid around the fusion neck between the fused vesicles. The restoring force is related to the bending elasticity of the lipid bilayer. The corresponding decay time in this later stage can be presented as $\tau_{late} \sim \eta \Delta V/\kappa$, where η is the bulk viscosity of

sucrose/glucose solution, $\Delta V \sim R^3$, and κ is the bending elasticity modulus of the membrane. For egg-PC $\kappa \approx 10^{-19}$ J (4, 5). Thus for a typical vesicle size of R = 20 μm, we obtain $\tau_{late} \sim 100$ s which is the time scale that we measure for complete fusion neck opening.

Supporting movies

Supporting Movie S1. Fusion of two functionalized vesicles (25.4 μm and 16.6 μm in radius) held by micropipettes. The movie corresponds to the sequence presented in Fig. 1a. The actual length of the movie in lab time is 4.750 ms. The movie was slowed down 1000 times.

Supporting Movie S2. Fusion of two functionalized vesicles held by micropipettes (same event as in Movie S1 but slowed down only 50 times). The actual length of the movie in lab time is 129 ms.

Supporting Movie S3. Electrofusion of a vesicle couple when exposed to a DC pulse in the absence of salt. The movie corresponds to the sequence presented in Fig. 1b. The amplitude of the DC pulse applied was 90 V (1.8 kV/cm), and its duration was 150 μs. The actual length of the movie in lab time is 2 s.

Supporting Movie S4. Electrofusion of a vesicle couple (29.0 μm and 26.5 μm in radius) in the presence of 1 mM NaCl in the exterior solution. The movie corresponds to the sequence presented in Fig. 1c. The amplitude of the DC pulse applied was 150 V (3 kV/cm), and its duration was 150 μs. The actual length of the movie in lab time is 2 s.

Chemical structure of the β-diketone ligand.

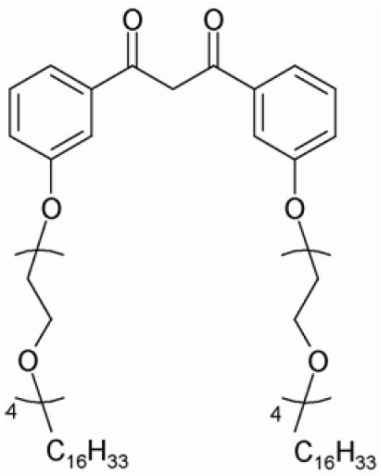

References

1. Kinosita, K., Ashikawa, Jr., I., Saita, N., Yoshimura, H., Itoh, H., Nagayama K. & Ikegami, A. (1988) *Biophys. J*. 53, 1015-1019.

2. Hochmuth, R., Shao, J.-Y., Dai, J. & Sheetz, M. (1996) *Biophys. J*. 70, 358–369.

3. Brochard-Wyart, F., de Gennes, P.G. & Sandre, O. (2000) *Physica A*. 278, 32–51.

4. Mutz, M. & Helfrich, H. (1990) *J. Phys. France*, 51, 991–1002.

5. Schneider, M.B., Jenkins, J.T. & Web, W.W. (1984) *Biophys. J*. 45, 891–899.